On the Combined Use of UVA, HALS, Photooxidation, And Fracture Energy Measurements to Anticipate The Long-Term Weathering Performance of Clearcoat/Basecoat Automotive Paint Systems

J.L. Gerlock, A.V. Kucherov,† and M.E. Nichols—Ford Motor Company*

INTRODUCTION

This work is a culmination of a long-standing research program designed to develop methods to quickly identify automotive paint systems that will exhibit superior long-term weathering performance. The research program is based on the premise that the long-term weathering performance of automotive paint systems is determined primarily by their ability to resist photooxidative degradation.[1-4] Accordingly, a number of analytical techniques have been examined to assess the photooxidation behavior of clearcoat/basecoat paint systems and the additives that influence photooxidation.

Analytical techniques have been reported in previous work to quantify generic photooxidation for isolated clearcoat films (transmission FTIR[5]), to quantify the photooxidation of the top 8-12 µm of clearcoat surface for clearcoats in complete paint systems (photoacoustic FTIR[6]), and the progress of photooxidation across all coating layers in complete paint systems ($^{18}O^-$-TOF-SIMS with ~2µm resolution.[7]) Techniques have also been reported to quantify ultraviolet light absorber (UVA) additive loss rates for isolated clearcoat films, transmission UV,[8,9] and UVA loss rates for clearcoat in complete paint systems with ~5µm resolution, micro-UV spectroscopy.[10] More recently, a technique has been reported to map the disposition of hindered amine light stabilizer (HALS) additives as "Active HALS" across all coating layers in complete paint systems with ~5µm resolution.[11,12] Techniques have also been developed to determine the fracture energy of clearcoats in clearcoat/basecoat paint systems.[13-15]

The present work applies the transmission FTIR spectroscopy photooxidation analysis, transmission UV spectroscopy UVA analysis, and the ESR spectroscopy Active HALS analysis techniques noted previously to 5 µm thick paint system slices obtained by in-plane microtomy of complete paint systems on standard steel test panels. Analysis results reveal the progress of photooxidation across all coating layers, clearcoat UVA disposition, and the disposition of HALS in clearcoat and basecoat layers as a function of outdoor exposure. These analysis results are combined with clearcoat fracture energy measurements of the mechanical repercussions of photooxidative degradation to allow an informed opinion to be formulated about the long-term weathering performance of clearcoat/basecoat paint systems.

Transmission UV spectroscopy measurements of clearcoat ultraviolet light absorber (UVA) disposition, electron spin resonance (ESR) spectroscopy measurements of clearcoat and basecoat Active hindered amine light stabilizer (HALS) disposition, and transmission Fourier transform infrared (FTIR) measurements of photooxidation have been carried out on 5 µm thick slices of clearcoat/basecoat/primer/e-coat paint systems on steel panels as a function of outdoor exposure. These analysis results are combined with clearcoat fracture energy measurements to assess the possibility that a clearcoat/basecoat paint system will resist catastrophic cracking/peeling failure at long times. Taken together, all results indicate that these nontraditional paint weathering performance metrics should be added to the existing repertoire of paint weathering performance metrics to ensure that inferior clearcoat/basecoat automotive paint systems are not introduced into service.

The first use of in-plane microtomy to examine automotive paint systems was reported by Bohnke et al.[16] These researchers used chromatography to assay 2 µm thick

*Ford Research Laboratory, MD 3182 SRL, P.O. Box 2053, Dearborn, MI 48124.
†Visiting Scientist; Zelinsky Institute of Organic Chemistry, RAS, Moscow, Russia.

paint system slices to examine the migration of UVA and HALS additives between coating layers during wet-on-wet clearcoat/basecoat cure. The same techniques were used to examine the behavior of UVA and parent HALS additives as a function of weather exposure. Clearcoat UVA was found to decrease with exposure. Parent HALS, specifically the HALS added to a paint system, was found to decrease rapidly as it was converted to inhibition cycle products. No attempt was made to assay inhibition cycle products, "Active HALS," to determine the amount of inhibition cycle products available to inhibit oxidation at long exposure times. Haacke et al. reported the use of in-plane microtomy to obtain T_g and crosslink density profiles for paint systems as well as to follow UVA migration during cure.[17] Adamsons et al. reported the use of FTIR spectroscopy measurements on 10 µm thick paint system clearcoat slices to produce depth profiles of chemical change for clearcoat/basecoat paint systems as a function of exposure.[18]

In the present work, ~5 µm thick paint system slices are analyzed for UVA content, Active HALS content, and degree of photooxidation. The results from sequentially weathered test panels are combined to reveal trends in the behavior of each of these weathering performance metrics as a function of exposure. Fracture energy measurements are carried out on strips cut from the same test panels to reveal trends in the mechanical performance as a function of exposure. It is claimed that the results of UVA, HALS, photooxidation, and fracture energy analysis obtained for relatively short-term exposure test panels, zero to five years exposure, can reveal trends in the behavior of these weathering performance metrics that allow the long-term weathering performance, >10 years, of clearcoat/basecoat/primer/e-coat paint systems to be anticipated.

EXPERIMENTAL

Chemicals

Spectroscopic grade CH_2Cl_2 was obtained from Fisher Scientific. *p*-Nitroperbenzoic acid (92% pure) was obtained from ICN Biomedicals Inc. From Aldrich Chemical, 4-hydroxy-2,2,6,6-tetramethylpiperidinyl-N-oxyl (TEMPOL) was obtained and recrystallized from hexane prior to use as a primary nitroxyl radical standard. Perfluorinated oil was obtained from M. W. Kellogg Co., Jersey City, NJ.

Paint Systems

Three paint systems on 4 × 12 in. steel panels were studied in the present work. They are designated G, B, and I. Results for paint system B have been reported in previous work.[11,12] In all cases, clearcoat was cured wet-on-wet over basecoat so that diffusion of HALS, UVA, and other lower molecular weight species between coating layers is expected during cure.

Paint System G: Paint System G consists of an acrylic/urethane clearcoat stabilized with 1% by wt Tinuvin 440 HALS (22.9 µmol of nitroxyl radical precursor/g clearcoat) and an oxanilide UVA over HALS-free, dark brown basecoat over primer over e-coat. Test panels were weathered in southern Florida and withdrawn after one, two, four, and five years of exposure. A nonexposed "retain" test panel was available.

Paint System B: Paint System B consists of an acrylic/urethane clearcoat stabilized with 1% by wt Tinuvin 292 HALS (39.4 µmol of nitroxyl radical precursor/g clearcoat) and a benzotriazole UVA over HALS-free, black basecoat over primer over e-coat. Test panels were weathered in northern Australia and withdrawn after one, three, and four years of exposure. All test panels including the retain test panel were subjected to one month of additional exposure in Michigan during the month of August 1998 to reestablish steady-state nitroxyl radical concentration after prolonged storage in the dark. It is not clear that this additional exposure was necessary.

Paint System I: Paint System I consists of an acrylic/melamine/silane clearcoat stabilized with 1.43% by wt Tinuvin 123 HALS (38.8 µmol of nitroxyl radical precursor/g clearcoat) and a benzotriazole UVA over white, HALS-free, waterborne basecoat over primer over e-coat. Test panels were weathered in southern Florida and withdrawn after one, three, and five years of exposure. A nonexposed retain test panel was available.

In-plane Microtomy: Sample slices measuring 1in. × 1.2 in. × ~5 µm were cut using a Polycut E microtome, Leica SM2500 E, Cambridge Instruments GmbH.

In a typical experiment, a 4 × 8 × 1.5 in. block of polypropylene was placed in the microtome's sample holder and the surface of the block was microtomed flat using a tungsten carbide blade with a 50° cutting angle. Next, a ~1.2 × 3 in. section of flat test panel was cut from a 4 × 12 in. test panel using a diamond wheel and the panel section was glued to the surface of the polypropylene block with double-sided adhesive paper. The cutting blade was advanced toward the sample surface in 1 µm increments at a cutting speed of 3-4 mm/sec until the blade made contact with the surface. Upon contact, the cutting increment was increased to 5 µm. A typical paint system yields 18-22 ~5 µm thick coating slices.

Analytical Procedures

Sample slices were analyzed in the following sequence: transmission UV spectroscopy, followed by transmission FTIR spectroscopy, followed by ESR spectroscopy. Finally, strips were cut from the nonmicrotomed portion of the steel panels for fracture energy analysis.

UVA Analysis: In most cases, coating slices were not sufficiently transparent to provide useful UV spectra due to light scattering. However, when the slices are wetted with a perfluorinated oil, light scattering decreases from >0.7 to <0.3 in the 450 nm region.

In a typical UVA analysis, a ~5 µm thick coating slice measuring ~1.0 × 1.2 cm was wetted with perfluorinated oil, fixed between 25 mm diameter NaCl plates, and placed in a CO550303 sample holder (Perkin Elmer). The UV spectrum of each slice was recorded over the 250-450 nm range in absorbance mode using a Perkin Elmer UV/VIS Lambda 18 spectrometer. A baseline spectrum was recorded for NaCl plates wetted with perfluorinated oil. Generally, light scattering by basecoat, primer, and e-coat pigments is too intense to obtain useful UVA spec-

tra. The presence or absence of UVA can be noted, but not quantified.

UV spectra could not be recorded for the clearcoat/basecoat interface region for four and five-year exposure paint system G test panels because microtomy produced a powder.

PHOTOOXIDATION ANALYSIS: While light scattering is much less severe for IR than UV spectroscopy, wetting samples with perfluorinated oil does reduce the baseline in the 4000-2000 cm^{-1} region. Strong absorbance peaks due to perfluorinated oil are observed in the 1300-1100 cm^{-1} region, but do not interfere with (–OH, –NH)/–CH ratio measurements in the 4000-2000 cm^{-1} region.

In an ancillary experiment, (–OH, –NH)/–CH ratio measurements on dry samples and samples wetted with perfluorinated oil produced identical results for two sets of 18 paint system G samples. This indicates that coating slices wetted with perfluorinated oil to reduce light scattering for UV spectroscopy measurements can also be used for transmission FTIR spectroscopy measurements.

In a typical FTIR analysis, the NaCl plates with coating slices were placed in an FTIR sample holder, and spectra were recorded over the 4000-600 cm^{-1} range using a Matteson Galaxy Series FTIR 5000 spectrometer. A baseline spectrum was recorded for NaCl plates wetted with perfluorinated oil. In most cases, scattering by pigments was sufficiently low for 5 µm thick slices to allow reasonable IR spectra to be recorded for all coating layers. Spectra were manipulated using WIN-FIRST software.

As previously noted, intact slices could not be obtained for the interface region of four and five-year exposure paint system G test panels. Microtomy produced a powder. The powder was ground with one drop of perfluorinated oil in an agate mortar and the IR spectrum of the mull was recorded between NaCl plates. Trial experiments wherein intact films were treated in the same manner indicate that the same (–OH, –NH)/–CH ratio value is obtained for free standing films and material dispersed in perfluorinated oil.

The contribution of absorbed water to 4000-2000 cm^{-1} region absorbance was examined by comparing the FTIR spectra of samples immediately after microtomy in the open air with spectra for slices dried at 80°C for two hours. No measurable difference was detected.

HALS ANALYSIS: ESR instrumentation and techniques have been described in detail in previous work.[11,12] Briefly, ESR spectra are recorded for CH_2Cl_2 swelled dispersions of coating samples in 3mm ID, thin walled quartz samples tubes at the following spectrometer settings: sweep width = 170 G, modulation = 2 G, and power = 6.4 mW.

In practice, 5-10 mg of coating is loaded into the ESR sample tube, weighed, and 0.2-0.3 ml of CH_2Cl_2 is added. The mixture is stirred with a fine glass rod for approximately two minutes and then immersed in an ultrasonic bath for 30 sec to produce a uniform dispersion. After sonication, the sample tube is closed and reweighed to determine the amount of CH_2Cl_2 present. The ESR spectrum of the dispersion is recorded to determine the steady-state concentration of nitroxyl radical, >$NO^{\cdot}$, prior to peracid oxidation. Next, 0.5-1 mg of *p*-nitroperbenzoic acid is added to the sample tube, the dispersion is stirred with a fine glass rod, and sonicated for 10 sec. Finally, the ESR spectrum of the sample is recorded periodically over a ~40 min period. The maximum nitroxyl radical signal intensity observed is used to calculate Active HALS concentration as µm moles of nitroxyl radical per gram of clearcoat.

Nitroxyl radical standards were prepared by dissolving known amounts of TEMPOL in CH_2Cl_2. The ESR spectrum of standard solutions were recorded in the same quartz samples tubes used for sample analysis. Linear plots were obtained for ESR signal double integral area versus TEMPOL concentration over the concentration range 0.1-10 µmol/g of CH_2Cl_2 solvent.

Fracture Energy Measurements

The fracture energy, a measure of a material's brittleness, was measured for each clearcoat using techniques that have been described in detail elsewhere.[13-15] Briefly, 8 mm strips were cut from the width of standard 4 × 12 in. steel test panel with a hand shear. The paint panel strips were then pulled in tension at 20 mm/min in a mechanical testing machine (Instron model 5565). The strain at which the clearcoat cracked was recorded. Multiple samples were tested for each panel at each weathering time. The fracture energy, G_c, was then calculated using the expression:

$$G_c = 0.5\pi h \varepsilon^2 \overline{E}_f g(\alpha,\beta) \quad (1)$$

where ε is the strain at cracking, h is the clearcoat thickness, $\overline{E}_f$ is the biaxial modulus of the clearcoat, and $g(\alpha,\beta)$ is a constant related to the mismatch in modulus between the coating and substrate. The modulus of the coating was previously determined from tensile testing on free films of similar clearcoats.

RESULTS AND DISCUSSION

It is generally agreed that photooxidative degradation plays a key role in determining the long-term weathering performance of clearcoat/basecoat automotive paint systems. Clearcoat photooxidation can lead to clearcoat cracking failure while the photooxidation of underlying coating layers can lead to peeling failure. In practice, a combination of both failure modes is usually observed and both leave no recourse other than to remove all coating layers and repaint in order to repair. In most cases, traditional weathering performance metrics, gloss loss, and color fading measurements, for example, provide little indication that catastrophic failure is imminent. Four nontraditional paint-weathering performance metrics are studied in the present work. These metrics are:

1) The ability of all coating layers in multilayer paint systems to resist photooxidative and hydrolytic degradation.

2) The ability HALS additives have to suppress the photooxidation of all coating layers in combination with the period of time that suppression is sustained.

3) The ability of clearcoat UVA to screen clearcoat and underlying coating layers from UV radiation that drives photooxidation in combination with the period of time that screening is sustained.

4) Clearcoat fracture energy—the ability of the clearcoat in a complete paint system to resist crack propagation.

Each of these weathering performance metrics is intimately linked to all others.

Photooxidation changes an organic coating's chemical composition. In the case of clearcoat/basecoat paint systems, photooxidation of the clearcoat's surface can lead to gloss loss when degraded clearcoat erodes away to expose hard particles, fused silica flow control additives for example that can scatter light. Photooxidation of the clearcoat's surface can cause the surface to embrittle and increase the likelihood of paint system failure by clearcoat cracking. And finally, photooxidation of the interfaces between clearcoat, basecoat, primer, and e-coat layers can lead to paint system failure by peeling when adhesion is destroyed. It is therefore necessary to follow the progress of photooxidation across all coating layers in multilayer paint systems in order to assess the impact of photooxidation on long-term weathering performance. Surface restricted photooxidation measurement techniques, such as photoacoustic and attenuated total reflectance FTIR spectroscopy, cannot afford adequate information to evaluate long-term weathering performance for the same reasons that gloss measurements do not afford adequate information. In the present work, transmission FTIR spectroscopy is used to map the progress of photooxidation (and hydrolysis) across all coating layers in complete paint systems as a function of exposure, through measurements on individual paint system slices.

HALS and UVA measurements are carried out on the same paint system slices in order to relate the photooxidation behavior observed to additive performance. The performance of HALS and UVA additives can play an important role in determining long-term weathering performance because most automotive paint systems employ polymers that rely on HALS and UVA additive performance to achieve photooxidation resistance.[19] When HALS and UVA additives are used to promote photooxidation resistance, the physical location of the additives within the paint system, the ability of the additives to inhibit photooxidation, and the period of time that each additive remains effective can provide insight into long-term weathering performance. For example, while the actual impact of a HALS on the weathering performance of a paint system cannot be evaluated without photooxidation, fracture energy, and perhaps gloss data, inferior HALS performance can be an early indicator that a paint system could exhibit inferior weathering performance. A superior HALS will be physically located within a paint system where photooxidation is likely to occur, inhibit photooxidation, increase UVA longevity,[5] and sustain the inhibition for an extended period of time. An inferior HALS will perform otherwise. In the present work, peracid oxidation is used to convert parent HALS and its inhibition cycle products to nitroxyl radicals that can be quantified by ESR spectroscopy to map the disposition of Active HALS across all coating layers in complete paint systems as a function of exposure.

In the same fashion, the impact of a UVA on the weathering performance of a paint system cannot be assessed in the absence of photooxidation, fracture energy, HALS longevity, and perhaps gloss and color fade data, but

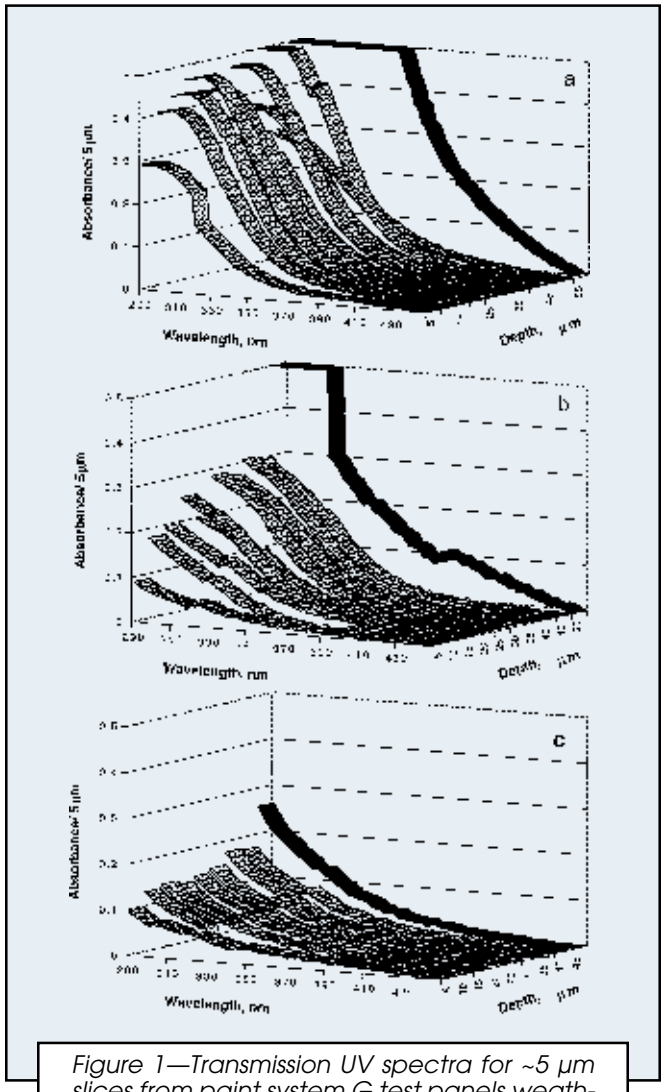

Figure 1—Transmission UV spectra for ~5 µm slices from paint system G test panels weathered in southern Florida for (a) zero, (b) one, and (c) two years.

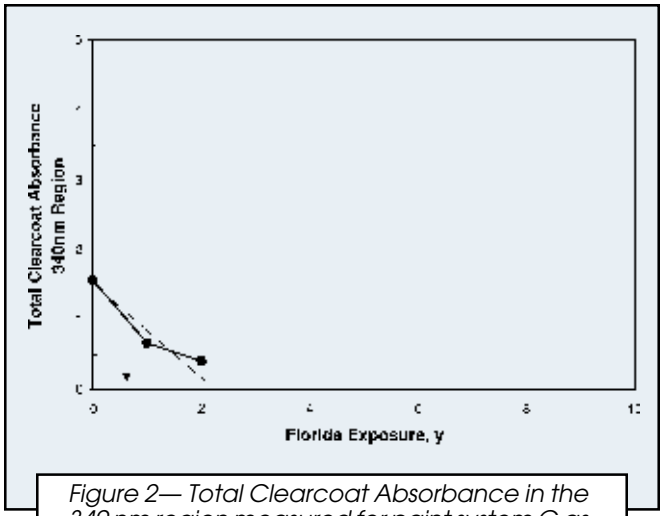

Figure 2— Total Clearcoat Absorbance in the 340 nm region measured for paint system G as a function of southern Florida exposure.

inferior UVA performance can be an early indicator that a paint system could exhibit inferior weathering performance. A superior UVA will be physically located within a paint system where is can absorb UV radiation capable of driving photooxidation, and sustain the screening effect for an extended period of time. An inferior UVA will perform otherwise. Transmission UV spectroscopy is used to map the disposition of UVA in the clearcoats in complete paint systems in the present work. Light scattering by pigments prevents the direct measurement of the UVA content of other coating layers.

Clearcoat fracture energy measurements provide a means to assess a paint system's susceptibility to failure by cracking. The fracture energy of a clearcoat in a complete paint system invariably changes with weather exposure. While the direction of change is almost invariably towards lower values of fracture energy, the rate of change appears to be linked to the balance struck between crosslink scission and crosslink formation reactions and the nature of the crosslinks involved. The factors that control the balance are not well understood for different coating chemistries. For example, it has only recently been demonstrated that HALS can reduce crosslink formation in acrylic/melamine clearcoats[20] and that comparable amounts of photooxidation need not produce comparable fracture energy changes in chemically different clearcoats.[21] These observations make it clear that relationships between weather-induced chemical composition changes and fracture energy changes are too poorly developed to allow the behavior of one to be inferred from the behavior of the other. This is unfortunate because extended exposure is usually required to make trends in fracture behavior sufficiently obvious to deduce a paint system's susceptibility to cracking failure. However, extended exposure is not always required. Clearcoats whose fracture energy is quite low before exposure, may crack after very limited exposure when subjected to the hygrothermal stresses typically imposed by outdoor exposure conditions. These stresses give rise to crack driving energies on the order of ~25 J/m^2 in standard thickness (~50 µm) clearcoats. All clearcoats, regardless of exposure time, are susceptible to cracking failure when their fracture energy approaches this level.[21]

In the sections that follow, trends in UVA, HALS, photooxidation, and fracture energy weathering performance metrics are used to identify clearcoat/basecoat paint systems whose long-term weathering performance is likely to be flawed. Analysis results are used to illustrate behaviors, not select the superior paint system within a series paint system candidates. Accordingly, the chemical composition of the paint systems, the nature of the additive packages employed, how each paint system was applied, and the fact that the paint systems were exposed at different times, for different amounts of time at different locations is unimportant for illustration purposes. It is disappointing that all test panels were withdrawn from exposure before catastrophic failure was observed, but this was the practice when the test panels were generated. As a result, the validity of the proposed weathering-performance metrics is not directly confirmed by outdoor exposure results. It can be noted, however, that every failed-in-service paint system studied in our laboratory to date exhibits inferior performance in at least one of the weathering performance metrics studied here and usually all. The fact that 10-year exposure panels do not exist for paint systems studied in the present work is not unusual. In fact, it represents the norm in practice. Neither paint companies nor their customers could operate in an environment that demanded 10 or even five-year outdoor exposure results before making decisions to: (a) introduce modified paint systems to cope with changing solvent emissions regulations, (b) change HALS and/or UVA additives in existing paint systems to take advantage of new developments in additives research, (c) change paint application procedures to improve efficiency and/or reduce costs, (d) change pigments and/or coating layer arrangements to improve appearance and/or reduce costs, (e) paint new substrates, or (f) to substitute one coating chemistry for another in existing paint systems to cope with supply changes. Under these conditions, a series of weathering performance metrics whose behavior can reduce the possibility of introducing

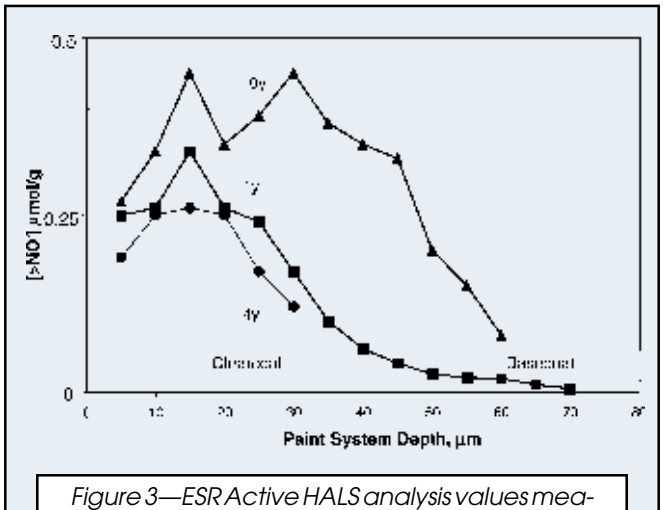

Figure 3—ESR Active HALS analysis values measured for ~5 µm slices from paint system G test panels weathered in southern Florida for zero, one, and four years.

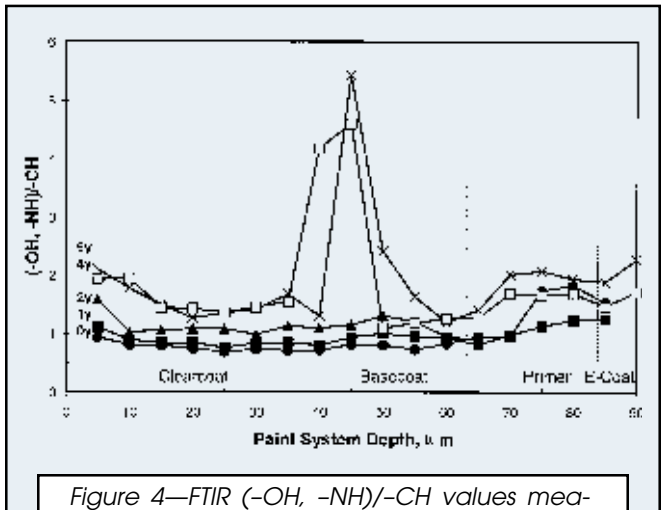

Figure 4—FTIR (–OH, –NH)/–CH values measured for ~5 µm slices from paint system G test panels weathered in southern Florida for zero, one, two, four, and five years.

paint systems that could perform poorly in service is valuable. No attempt has been made to use the metrics studied here to calculate absolute service life.

Paint System G

UVA Analysis: Paint system G UVA analysis results are shown in *Figure* 1a, b, and c for zero, one, and two-year exposure test panels respectively. It is noted that the absorbance curves are not as well behaved as those obtained by micro-UV spectroscopy.[10] This is no doubt due to the fact that an absolute measurement is being carried out on sample slices whose thickness varies around the five µm value intended. Nevertheless, the curves are entirely adequate to estimate UVA longevity. UVA longevity can be estimated by summing absorbance values at any wavelength to yield a Total Clearcoat Absorbance value. The results of this treatment shown in *Figure* 2 suggest that ~45 µm of paint system G clearcoat will limit the transmission of 340 nm UV radiation to underlying basecoat to <10% for <1 year. This estimate will be higher or lower in practice depending on actual clearcoat thickness. The result indicates that the clearcoat in paint system G will expose underlying basecoat to UV radiation after several years of exposure. This behavior does not in itself constitute a paint system flaw. The behavior is however recognizable after only two years of exposure. As will be shown shortly, photooxidation measurements clearly reveal that the basecoat in paint system G is sensitive to UV radiation and limited clearcoat UV screening in combination with UV radiation sensitivity does constitute a paint system flaw.

The analysis of a non-exposed section of test panel shielded from sunlight by exposure rack clamps for five years indicates minimal UVA loss. This suggests that the root cause of UVA loss may be chemical destruction as opposed to physical loss.

Active HALS Analysis: Paint system G Active HALS analysis results are shown in *Figure* 3 for zero, one, and four-year exposure tests panels. The low Active HALS analysis result obtained for the nonexposed test panel is not unexpected. Tinuvin 440 HALS is not readily oxidized to nitroxyl radical by *p*-nitroperbenzoic acid in CH_2Cl_2. The low results obtained for one and two-year exposure test panels are also not unexpected because previous work has shown that Tinuvin 440 is not readily converted to inhibition cycle products during outdoor exposure[11] or during artificial light exposure that closely approximates sunlight.[22] Paint system G is known to perform well in QUV FS-40 accelerated weathering tests. Here the wavelength distribution of the fluorescent light source closely matches the absorbance spectrum of oxanilide UVA used and Tinuvin 440 does inhibit photooxidation. Of course the results of such accelerated weathering tests need have little bearing on actual weathering performance.

The absence of substantial concentration of Active HALS need not mean that Tinuvin 440 does not inhibit photooxidation in paint system G. Relationships between HALS concentration and effectiveness are not well understood. However, the absence of a substantial concentration of Active HALS does suggest that Tinuvin 440 is not readily converted to inhibition cycle products and may not be effective.

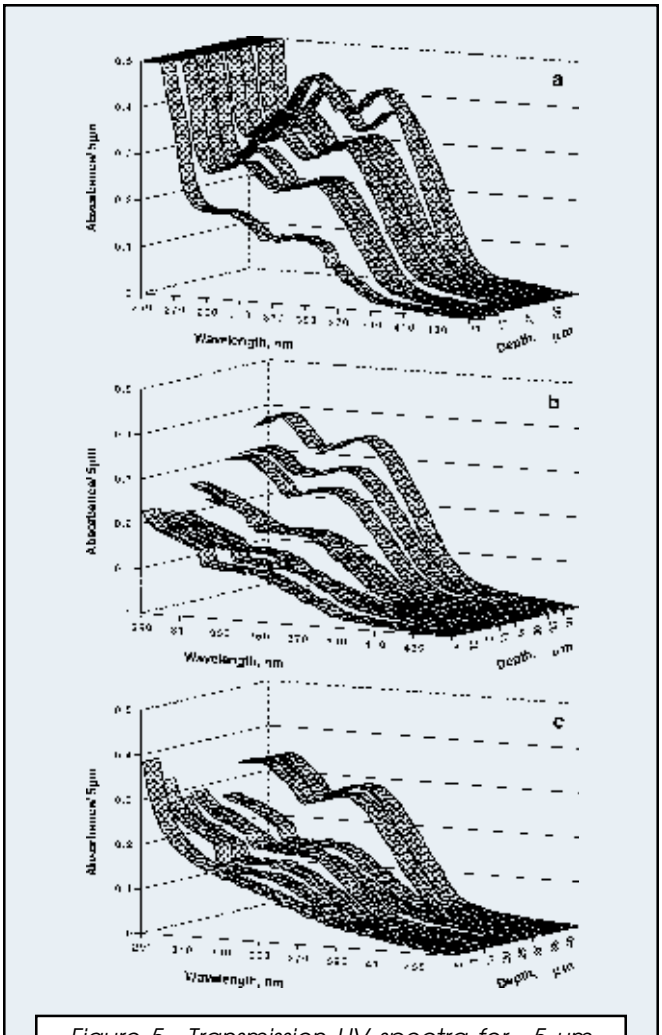

Figure 5—Transmission UV spectra for ~5 µm slices from paint system B test panels weathered in northern Australia for (a) one, (b) three, and (c) four years.

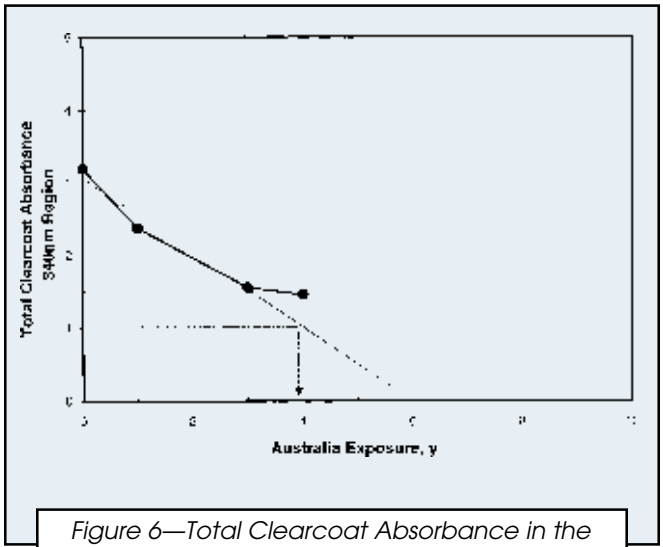

Figure 6—Total Clearcoat Absorbance in the 340 nm region measured for paint system B as a function of northern Australia exposure.

The steady-state concentration of nitroxyl radical present in paint system G clearcoat prior to peracid oxidation is below the detection limit of the ESR analysis technique, < 0.1 µmol/g of clearcoat.

Photooxidation Analysis: Paint system G photooxidation analysis results are shown in *Figure* 4 for zero, one, two, four, and five-year exposure test panels. Surface (–OH, –NH)/–CH peak area ratio values increase for one and two-year exposure panels, but there is no indication that the clearcoat bulk or the interface between the clearcoat and the basecoat is prone to photooxidation. At some point between two and four years of exposure, intense clearcoat/basecoat interface oxidation begins. The onset of rapid clearcoat/basecoat interface photooxidation parallels the depletion of clearcoat UVA. Taken together, UVA, Active HALS, and photooxidation weathering performance metrics clearly indicate and explain why paint system G could fail by clearcoat peeling after four to five years of outdoor exposure. Four and five-year exposure test panels do peel after water soak stress. The fact that the basecoat in paint system G is sensitive to UV radiation could have been recognized earlier had UVA-free test panels been exposed.

Clearcoat Fracture Energy Analysis: The fracture energy values measured for zero and two-year exposure panels, 1460 and 490 J/m^2 respectively, are not sufficient to ascertain whether paint system G is susceptible to cracking failure at long exposure times. Long-term fracture energy values are not available because intact sections of four and five-year exposure test panels that failed water soak were destroyed for photooxidation analysis.

Paint System G Summary

UVA measurements on zero, one, and two-year exposure panels indicate that the initial concentration of clearcoat UVA is low and decreases rapidly with exposure. Active HALS measurements on the same panels provide no evidence that an effective HALS is present. Photooxidation measurements on zero, one and two years exposure panels provide no evidence that clearcoat or the interface between clearcoat and basecoat is prone to photooxidation. However, photooxidation measurements on four and five-year exposure test panels clearly reveal that the clearcoat/basecoat interface does photooxidize rapidly when exposed to UV radiation. Fracture energy measurements on zero, one, and two-year exposure panels indicate that clearcoat fracture energy is initially high.

It can be noted that neither the physical appearance of the clearcoat on four and five-year exposure test panels nor surface region photooxidation measurements reveal that paint system G is flawed by a clearcoat/basecoat interface that is prone to photooxidation when ultimately exposed to UV radiation. This behavior illustrates a fundamental difference in the photooxidation behavior of monocoat and clearcoat/basecoat paint systems.

Paint System B

UVA Analysis: Paint system B UVA analysis results are shown in *Figure* 5a, b, and c for one, three, and four-year exposure test panels, respectively. When 340 nm region absorbance values are summed for individual clearcoat

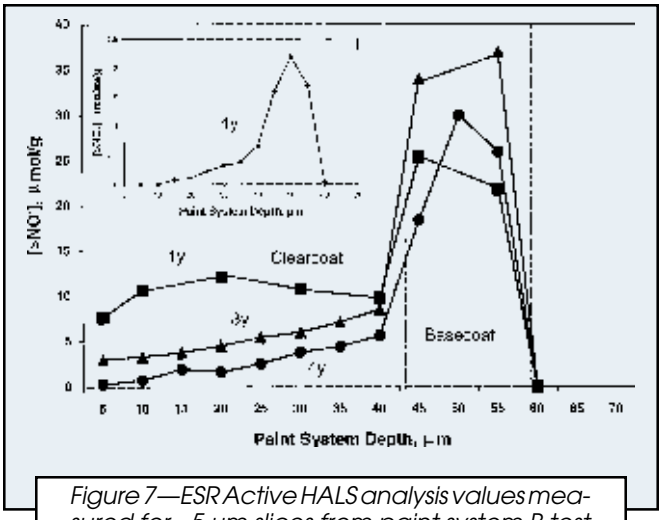

Figure 7—ESR Active HALS analysis values measured for ~5 µm slices from paint system B test panels weathered in northern Australia for one, three, and four years. Insert shows steady-state concentration.

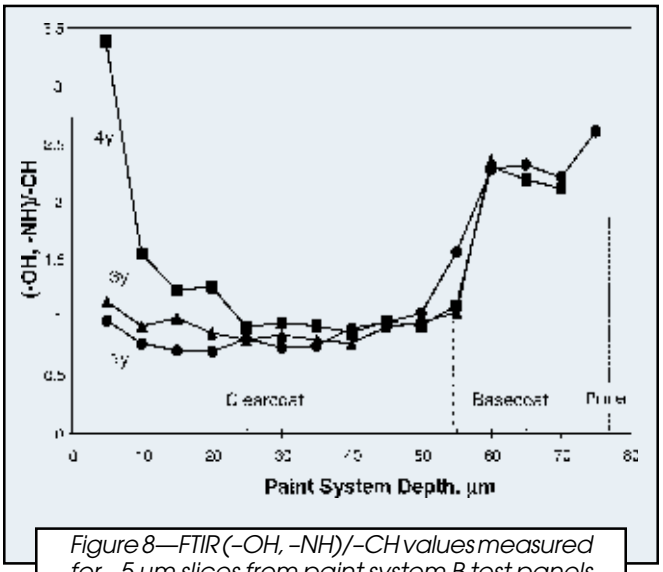

Figure 8—FTIR (–OH, –NH)/–CH values measured for ~5 µm slices from paint system B test panels weathered in northern Australia for one, three, and four years.

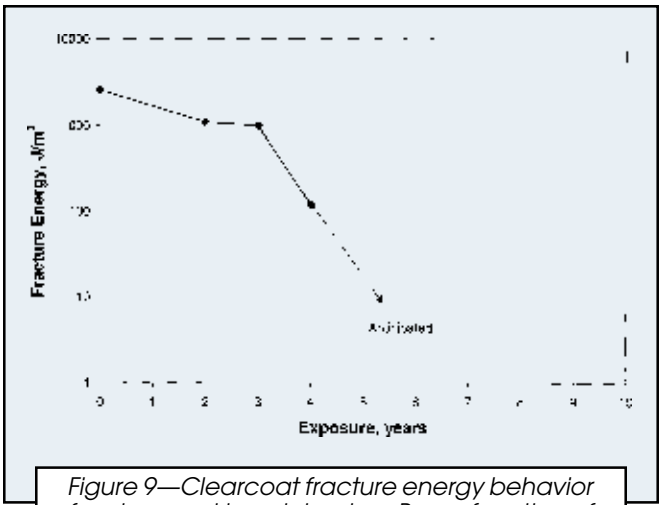

Figure 9—Clearcoat fracture energy behavior for clearcoat in paint system B as a function of outdoor exposure.

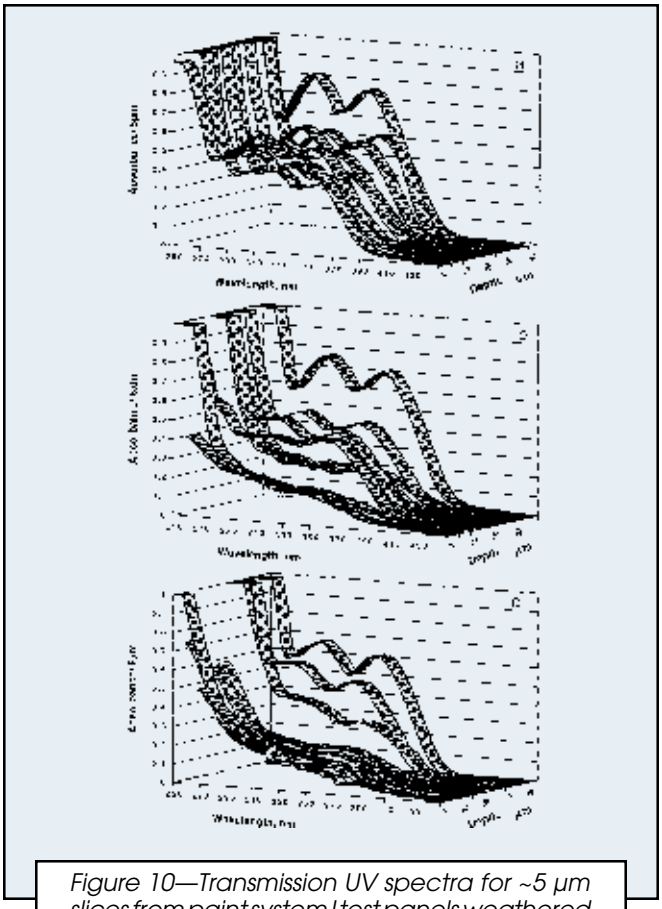

Figure 10—Transmission UV spectra for ~5 µm slices from paint system I test panels weathered in southern Florida for (a) one, (b) three, and (c) five years.

slices and combined with an estimate of the starting absorbance obtained from absorbance curves near the bottom of the one-year exposure test panel, the Total Clearcoat Absorbance versus exposure plot shown in *Figure* 6 is obtained. The plot indicates that the transmission of 340 nm region UV radiation will be limited to <10% for >4 years.

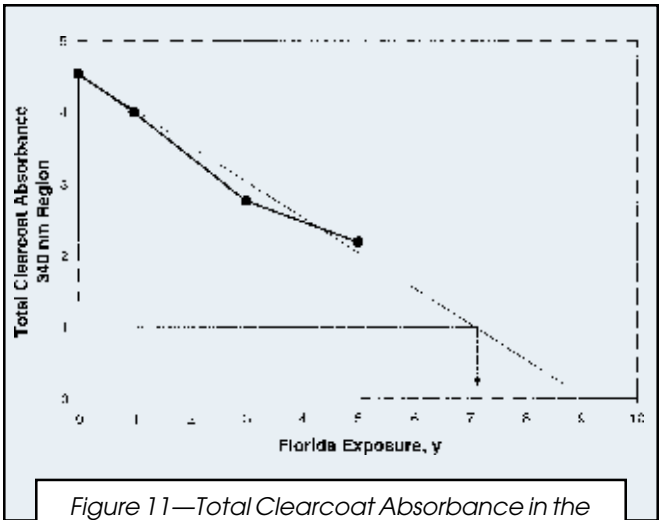

Figure 11—Total Clearcoat Absorbance in the 340 nm region measured for paint system I as a function of southern Florida exposure.

This estimate may be low because the clearcoat appears to yellow (curvature in plot after three years of exposure).

Active HALS Analysis: Paint system B Active HALS analysis results are shown in *Figure* 7 for one, three, and four-year exposure test panels. The results obtained for the one-year exposure test panel indicate that the HALS present in the clearcoat prior to cure migrates to the basecoat during cure. This behavior reduces the actual concentration of parent HALS in the clearcoat considerably prior to weather exposure. As exposure proceeds, the concentration of Active HALS in the surface region of the clearcoat decreases to a very low value. This suggests that the surface region of the clearcoat could revert to its HALS-free photooxidation rate at long exposure times.

Interestingly, the steady-state nitroxyl radical concentration profile obtained for the four-year test panel prior to peracid oxidation (insert in *Figure* 7), appears to provide, at least qualitatively, the same information about the disposition of HALS in the paint system as Active HALS analysis. This point will be noted again when results for paint system I are presented.

Photooxidation Analysis: Photooxidation analysis results are illustrated in *Figure* 8 for one, three, and four-year exposure test panels. Little or no change in (–OH, –NH)/–CH peak area ratio values is observed in the bulk of the clearcoat or at the clearcoat/basecoat interface region with exposure. However, the surface of the clearcoat begins to photooxidize rapidly after three years of exposure. Oxidation penetrates >10 µm into the clearcoat bulk. This behavior is consistent with the depletion of Active HALS and UVA in the surface region of the clearcoat.

Clearcoat Fracture Energy Analysis: Clearcoat fracture energy values are plotted versus exposure time in *Figure* 9. The results indicate that clearcoat fracture energy decreases rapidly after three and four years of exposure in sync with the onset of rapid clearcoat surface oxidation. Were this rate

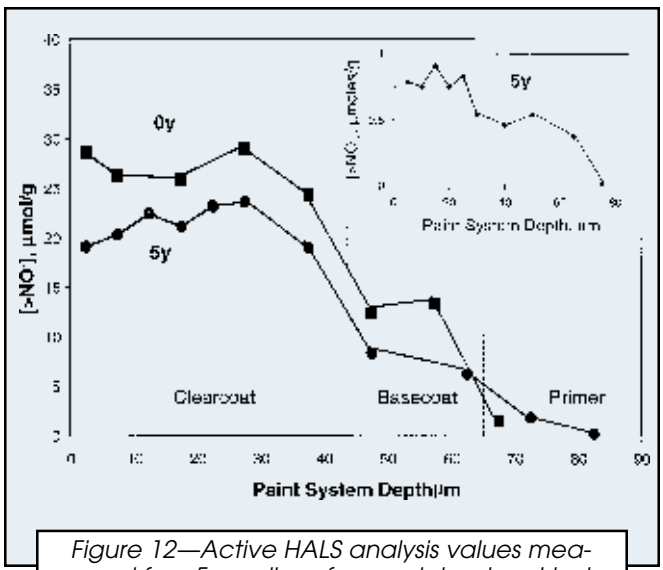

Figure 12—Active HALS analysis values measured for ~5 µm slices from paint system I test panels weathered in southern Florida for zero and five years. Insert shows steady-state nitroxyl concentration.

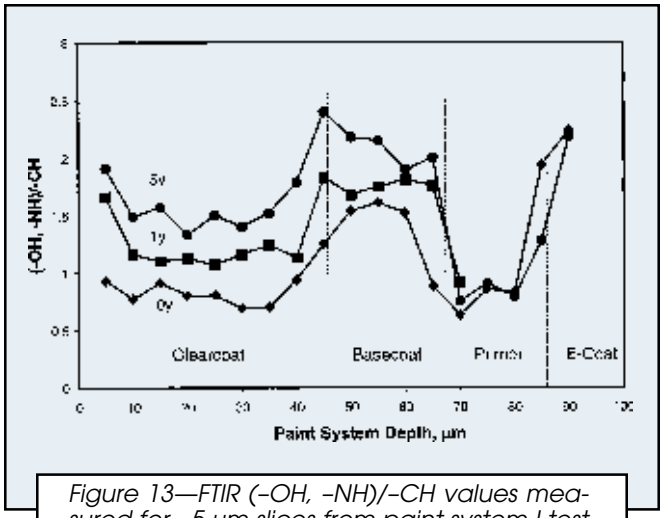

Figure 13—FTIR (–OH, –NH)/–CH values measured for ~5 µm slices from paint system I test panels weathered in southern Florida for zero, one, and five years.

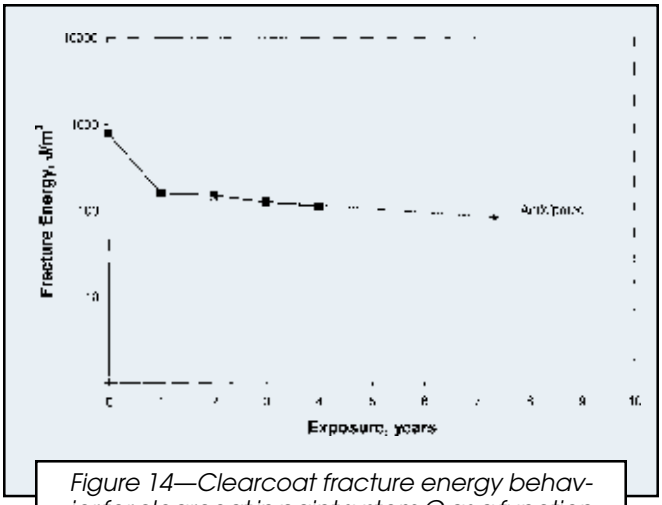

Figure 14—Clearcoat fracture energy behavior for clearcoat in paint system G as a function of outdoor exposure.

of embrittlement to continue, the clearcoat would cross the threshold value of 25 J/m^2 with only limited continued exposure.

Paint System B Summary

The results of UVA, Active HALS, photooxidation, and clearcoat fracture energy measurements indicate that depletion of clearcoat surface region UVA and HALS after three years of exposure coincides with the onset of rapid clearcoat photooxidation and a rapid decrease in clearcoat fracture energy. Taken together, these weathering performance metrics suggest that paint system B could fail by clearcoat cracking at long exposure times.

Paint System I

UVA Analysis: Paint system I UVA analysis results are shown in *Figure* 10a, b, and c for one, three, and five-year exposure test panels. The plot of Total Clearcoat Absorbance values versus exposure time shown in *Figure* 11 suggests that the clearcoat in paint system I will limit the transmission of 340 nm region UV radiation to underlying basecoat to <10% for >7 years.

Active HALS Analysis: Active HALS analysis results for paint system I are shown in *Figure* 12 for zero and five-year exposure test panels. The concentration of Active HALS in the clearcoat's surface and in the bulk of the clearcoat remains high after five years of exposure.

Again, it is of interest to note that the steady-state nitroxyl radical concentration profile observed for the five-year test panel (insert in *Figure* 12), appears to provide, at least qualitatively, the same information about the disposition of HALS in the paint system as Active HALS analysis results. This was also noted to be the case for paint system B.

Photooxidation Analysis: Photooxidation analysis results are shown in *Figure* 13 for zero and five-year exposure test panels. There is no evidence of intense clearcoat surface or clearcoat/basecoat interface oxidation. (–OH,–NH)/–CH peak area ratio values are uniformly higher for both clearcoat and basecoat layers after five years of exposure. Because clearcoat UVA should produce a gradient in clearcoat photooxidation, the uniform increase in (–OH, –NH)/–CH peak area ratio observed may arise from thermal oxidation and/or hydrolytic degradation. (–OH, –NH)/–CH peak area ratio changes need not distinguish between these chemistries.

Clearcoat Fracture Energy Analysis: Clearcoat fracture energy values are plotted versus exposure time in *Figure* 14. The results indicate that after an initially rapid decrease in the fracture energy, the fracture energy then plateaus and only slowly changes for the next three years. If this behavior were to continue, the clearcoat would not cross the threshold value of 25 J/m^2 before extended exposure. The initial rapid decrease in the fracture energy need not be associated with photooxidation, but can arise from completion of cure and loss of residual solvent during the initial stages of exposure. These effects are not likely to be observed using the other analysis techniques discussed in this paper, but can be quite evident in the mechanical performance of the clearcoat.

Paint System I Summary

UVA, Active HALS, photooxidation, and clearcoat fracture energy paint weathering performance metrics provide no indication that paint system I will not resist catastrophic failure at long times in service.

CONCLUSIONS

It is concluded that the addition of four nontraditional paint weathering performance metrics to the repertoire of traditional paint weathering performance metrics could dramatically reduce the possibility that inferior clearcoat/basecoat paint systems will be introduced into service. The nontraditional weathering performance metrics are: (1) clearcoat UVA performance, (2) clearcoat and basecoat HALS performance, (3) the ability of all coating layers to resist photooxidation, and (4) clearcoat fracture energy.

Analysis results for three commercial clearcoat/basecoat paint systems as a function of outdoor exposure support this conclusion.

References

(1) Wypych, G., *Handbook of Material Weathering*, 2nd Ed., Chem Tec Publishing, Ontario, Canada, 1995.

(2) Clough, R.L., Billingham, N.C., and Gillen, K.T. (Eds.), *Polymer Durability: Degradation, Stabilization, and Lifetime Prediction*, Advances in Chemistry Series 249, American Chemical Society, Washington, D.C., 1996.

(3) Hamid, S.H., Amin, M.B., and Maadhan, A.G. (Eds.), *Handbook of Polymer Degradation*, Marcel Dekker, Inc., New York, 1992.

(4) Bauer, D.R. and Martin, J.W. (Eds.), *Service Life Prediction of Organic Coatings: A Systems Approach*, ACS Symposium Series 722, American Chemical Society, Washington, D.C., Oxford University Press, 1999.

(5) Gerlock, J.L., Smith, C.A., Cooper, V.A., Dusbiber, T.G., and Weber, W.H, *Polym. Degrad. & Stab.*, 62 (2), 225-234 (1998).

(6) Carter, R.O. III, *Opt. Eng.*, 36 (2), 326-331 (1997).

(7) Gerlock, J.L., Prater, T.J., Kaberline, S.L., Dupuie, J.L., Blais, E.J., and Rardon D.E., *Polym. Degrad. & Stab.*, 65, 37-45 (1999).

(8) Pickett, J.E. and Moore, J.E., in: *Polymer Durability: Degradation, Stabilization, and Lifetime Prediction*, Clough, R.E., Billingham, N.C., and Gillen, T. (Eds.), ACS Advances in Chemistry Series 249, American Chemical Society, Washington D.C., pp 287-301 (1996).

(9) Gerlock, J.L., Smith, C.A., Nunez, E.M., Cooper, V.A., Liscombe, P., Cummings, D.R., and Dusbiber, T.G., *ibid.*, pp 335-347 (1996).

(10) Smith, C.A., Gerlock, J.L., and Carter, R.O. III, *Polym. Deg. & Stab.*, submitted for publication.

(11) Gerlock, J.L., Kucherov, A.V., and Matheson, R.R. Jr., *Polym. Deg. & Stab.*, in press.

(12) Gerlock, J.L. and Kucherov, A.V., *Polym. Deg. & Stab.*, submitted for publication.

(13) Nichols, M.E, Gerlock, J.L., Smith, C.A., and Darr, C.A. *Prog. in Org. Coat.*, 35, 153-159 (1999).

(14) Nichols, M.E., Darr, C.A., Smith, C.A., Thouless, M.D., and Fisher, E.R., *Polym. Deg. & Stab.*, 60, 291 (1998).

(15) Nichols, M.E., Gerlock, J.L., Smith, C.A., and Darr, C.A., *Prog. in Org. Coat.*, 35, 153 (1999).

(16) Bohnke, H., Avar, L., and Hess, E., "Analytical Studies of Light Stabilizers in Two-Coat Automotive Finishes," JOURNAL OF COATINGS TECHNOLOGY, *63*, No. 799, 53 (1991).

(17) Haacke, G., Brinen, J. S., and Larkin, P. J., "Depth Profiling of Acrylic/Melamine Formaldehyde Coatings," JOURNAL OF COATINGS TECHNOLOGY, *67*, No. 843, 29 (1995).

(18) Adamsons, K., Litty, L., Lloyd, K., Stika, K, Swartzfager, D., Walls, D., and Wood, B., in *Service Life Prediction of Organic Coatings: A Systems Approach*, Bauer, D.R. and Martin, J.W. (Eds.), ACS Symposium Series 722, Oxford University Press, pp. 257-287, 1999.

(19) Valet, A. in *Light Stabilizers for Paints*, Zorll, U. (Ed.), Vincentz Verlag, Hannover, Germany, 1997.

(20) Nichols, M.E. and Gerlock, J.L., *Polym. Deg. & Stab.*, 69, 197 (2000).

(21) Nichols, M.E. and Tardiff, J.L., *Proc. of the 2nd International Conference on Service Life Prediction of Coatings*, Monterray, CA, 1999, in press.

(22) Bauer, D.R., Gerlock, J.L., Mielewski, D.F., Paputa Peck, M.C. and Carter, R.O. III, *Polym. Deg. & Stab.*, 28, 39 (1990).